

# OPTIMAL LINEAR DETECTION OF SOQPSK

**Mark Geoghegan**  
Nova Engineering Inc., Cincinnati, OH

## ABSTRACT

Shaped Offset QPSK (SOQPSK), as proposed and analyzed by Terrance Hill, is a family of constant envelope waveforms that is non-proprietary and exhibits excellent spectral containment and detection efficiency. Detection results using the filtering found in conventional OQPSK demodulators have been published for two variants of SOQPSK, namely SOQPSK-A and -B. This paper describes a method of synthesizing an optimal linear detection filter, with regard to bit error probability (BEP), and presents the resulting performance.

## KEY WORDS

SOQPSK, Linear Receiver, Detection Efficiency

## INTRODUCTION

SOQPSK is a non-proprietary modulation technique that is quickly gaining popularity in both terrestrial and space applications. The family of SOQPSK waveforms, as described by Hill [1], are constant envelope signals with excellent spectral containment and detection efficiency. Performance results for two variants, namely SOQPSK-A and -B, were published. In addition to Hill's paper, analytical performance bounds for the optimal non-linear Viterbi detector for SOQPSK have been published [2] as well as performance results using both integrate and dump and third order Butterworth detection filters that are representative of current NASA ground and space OQPSK demodulator equipment [3].

The objective of this paper is to determine the detection performance attainable using a linear receiver structure to demodulate SOQPSK. Since SOQPSK is a family of waveforms with a wide range of signal characteristics, the 'best' filter is not likely to be of a single type and will be highly dependent on the individual member selected. Therefore, computer simulations were used to iteratively compute the optimal filter tap weights that yield the lowest bit error probability (BEP) for a given variant.

## DESCRIPTION OF SOQPSK

The SOQPSK waveforms described by Hill are constant envelope, continuous phase modulations that allow a designer to easily trade-off spectral and power efficiency by varying a few simple parameters. The waveforms are completely described by either their instantaneous phase or frequency. Figure 1 illustrates a conceptual SOQPSK modulator that maps a binary input stream  $a(i)$  into ternary valued (+1, 0, -1) frequency impulses  $\alpha(t)$ , passes them through a shaping filter with response  $g(t)$ , and applies the instantaneous frequency  $f(t)$  or phase  $\phi(t)$  to an appropriate modulator which produces the desired SOQPSK waveform.

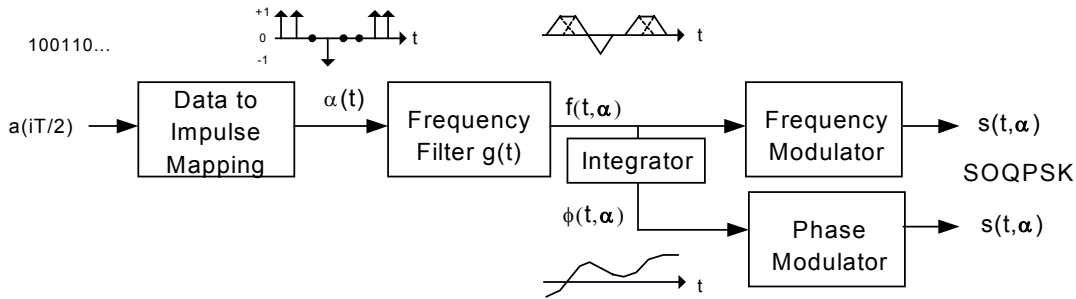


Figure 1. SOQPSK Modulator

The frequency pulse shapes for two variants of SOQPSK, which are called SOQPSK-A and SOQPSK-B, are given by  $g(t) = n(t) * w(t)$ , where

$$n(t) = \frac{A \cos(\pi \rho B t / T_s)}{1 - 4(\rho B t / T_s)^2} * \frac{\sin(\pi B t / T_s)}{(\pi B t / T_s)} \quad w(t) = \left. \begin{cases} 1, & \text{for } |t/T_s| < T_1 \\ \frac{1}{2} + \frac{1}{2} \cos \frac{\pi(|t/T_s| - T_1)}{T_2}, & \text{for } T_1 < |t/T_s| < T_1 + T_2 \\ 0, & \text{for } |t/T_s| > T_1 + T_2 \end{cases} \right\}$$

Note that  $T_s$  is the symbol period and that the four parameters  $\rho$ ,  $B$ ,  $T_1$ , and  $T_2$  serve to completely define the frequency pulse shapes for SOQPSK-A and SOQPSK-B, as well as an infinite set of similar, and interoperable, waveforms. The specific values for these SOQPSK variants are listed in Table 1 and the resulting pulse shapes and spectra are plotted in Figures 2 and 3. For comparison purposes, MIL-STD-188-182 SOQPSK, which uses a rectangular frequency pulse, is also included. The dramatic reduction in sidelobe energy makes SOQPSK-A and SOQPSK-B very attractive for terrestrial, satcom, and space applications.

Modulation Type	$\rho$	$B$	$T_1$	$T_2$
MIL-STD-188-182	0	0	0.25	0
SOQPSK-A	1.0	1.35	1.4	0.6
SOQPSK-B	0.5	1.45	2.8	1.2

Table 1. SOQPSK Parameters

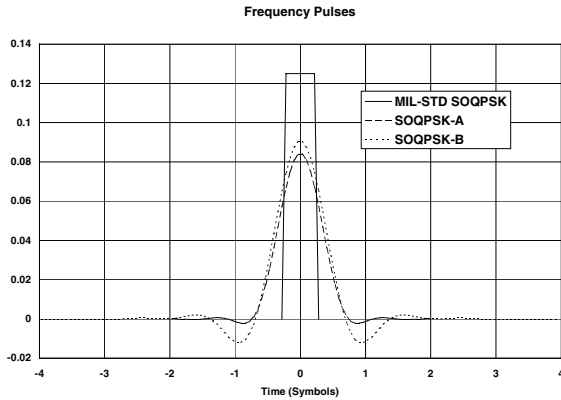


Figure 2. SOQPSK-A, -B Pulse Shapes

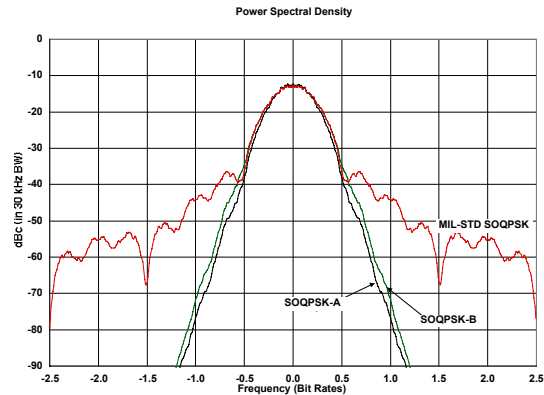


Figure 3. PSD of SOQPSK-A, -B

### LINEAR RECEIVER ARCHITECTURE

One method of demodulating SOQPSK consists of a linear filter followed by a sampler and a threshold comparator that recovers the data. A conceptual diagram of this architecture is shown in Figure 4. The signal is downconverted from a carrier frequency, filtered, and data decisions are made based on the peak samples of the filter outputs. The resulting odd and even data streams are recombined to produce the recovered data. Note that synchronization is assumed to be ideal. The only design issue in this architecture is the selection of the detection filter. The question becomes, “which detection filter gives the lowest bit error probability?” It is well known that the optimum detector for OQPSK is the integrate and dump filter. However, for SOQPSK, the ‘best’ filter is highly dependent on the characteristics of the individual member thereby requiring that the optimal filter be customized for each member. Therefore, the approach will be to synthesize a detection filter for a given variant using an iterative method to minimize bit error probability as the cost function.

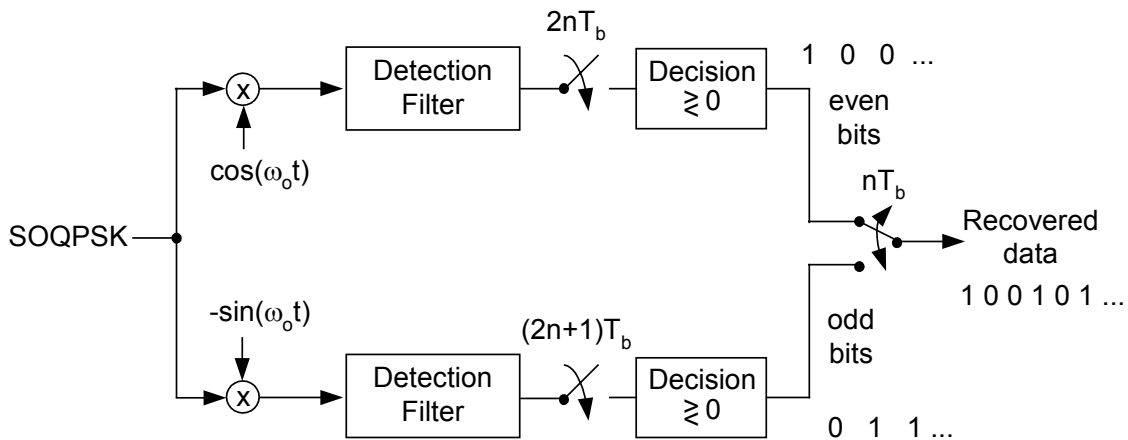


Figure 4. Conceptual Linear Receiver Architecture

## SYNTHESIS OF THE OPTIMAL DETECTION FILTER

The optimal filter tap weights for a given SOQPSK member can be determined using an iterative self-adapting algorithm. It is the same procedure that an adaptive equalizer uses to dynamically update the filter tap weights to equalize a distorted channel. However, in this case, the cost function is bit error probability. Figure 5 illustrates how the detection filter coefficients are updated. At each iteration, samples of the modulated waveform are filtered with the current tap weights and the resulting peak samples are extracted. The BEP is estimated by averaging the error probability of each peak sample given the statistics of the noise through the current filter. The calculated BEP is then compared to the previous BEP to form an error signal that adjusts the filter coefficients for the next iteration. This process continues until the filter converges. The tap weights are then declared 'optimum' and are used in the linear receiver structure in the previous section.

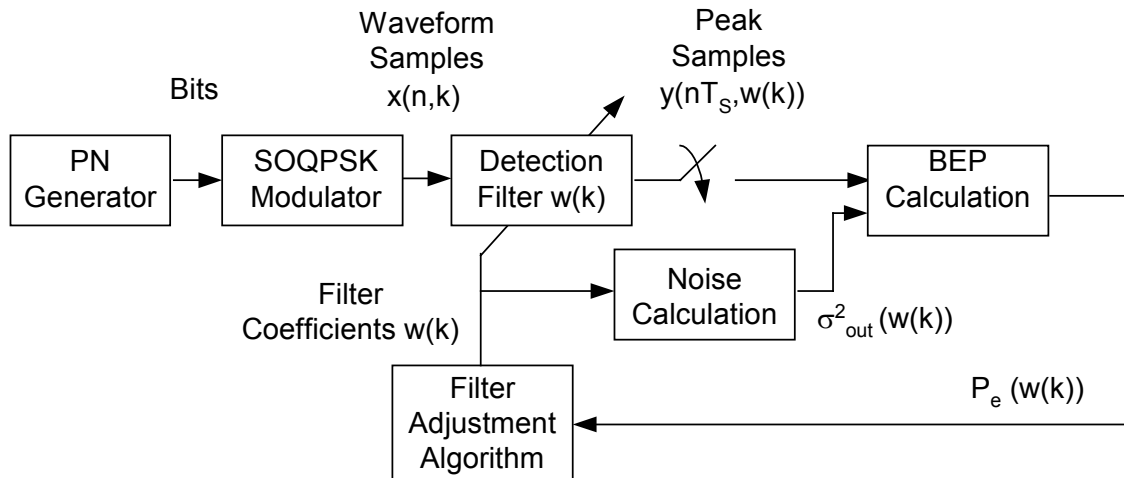


Figure 5. Process for Synthesizing an 'Optimal' Filter

At each iteration, the BEP for a given filter  $w(k)$  will be computed analytically using the desired  $E_b/N_0$ , the noise-free peak samples from the filter  $y(nT_s, w(k))$ , and the calculated variance of the noise at the filter output  $\sigma_{out}^2(w(k))$ . The noise and BEP calculations are performed using the equations listed below where  $\sigma_{in}^2$  is the noise variance at the input to the filter that would produce the desired  $E_b/N_0$  at which the filter is to be optimized. The noise variance at the filter output  $\sigma_{out}^2(w(k))$  is equal to the input variance  $\sigma_{in}^2$  multiplied by the sum of the squares of the filter taps. The bit error probability is the average of the individual error probabilities corresponding to each peak sample output.

$$\sigma_{out}^2(w(k)) = \sigma_{in}^2 \sum_{i=1}^L w(i, k)^2$$

$$P_e(w(k)) = \frac{1}{N} \sum_{n=1}^N \left( \frac{1}{2} \operatorname{erfc} \left( \frac{2|y(nT_s, w(k))|}{2\sqrt{2}\sigma_{out}(w(k))} \right) \right)$$

The filter adjustment algorithm uses a linear random-search technique [4] that tentatively adds a small random change to the tap weight vector and observes the change in performance. A permanent change is then made that is proportional to the product of the change in performance and the initial tentative change. The equation for updating the tap weights is shown below.

$$w(k+1) = w(k) + \frac{\mu}{\sigma_u^2} [P_e(w(k)) - P_e(w(k) + u(k))] \mu(k)$$

The terms  $P_e(w(k))$  and  $P_e(w(k)+u(k))$  are the error probabilities for the present and tentative tap weight values and  $u(k)$  is a random vector with variance  $\sigma_u^2$ . The constants  $\mu$  and  $\sigma_u^2$  affect the stability and rate of convergence. The behavior of this algorithm is similar to the steepest descent algorithm that searches in the direction of the gradient of the performance surface.

## PERFORMANCE RESULTS

The detection results for several SOQPSK variants are presented in this section. In addition to the ‘optimized’ linear detector, results for an integrate and dump and a Butterworth filter as well as the optimum non-linear Viterbi detector are included for comparison. The integrate and dump and the third order Butterworth filter (3 dB cutoff at the bit rate) are representative of the detectors used in NASA’s space and ground network conventional OQPSK demodulators. All bandwidth values are representative of operation with a non-linear amplifier (NLA).

Detection filters for four variants were synthesized; SOQPSK-A (1,1.35,1.4,0.6), -B (0.5,1.45,2.8,1.2), SOQPSK (0.7,1.25,1.5,0.5) which has the same bandwidth as -A but better detection efficiency, and SOQPSK (0.2,2.05,1.8,0.2) which requires slightly more bandwidth than either -A or -B but works very well with conventional Butterworth and integrate and dump filtering. Table 2 summarizes the simulation results with perfect synchronization and shows that additional gain in detection performance can be achieved by optimizing the detection filter. Improvements with the optimized filters range from 0.2 to 2.0 dB over the conventional detection filters. Although SOQPSK (0.7,1.25,1.5,0.5) has the same spectral efficiency as -A, its detection efficiency is 0.13 dB better with optimized filtering and 0.67 and 0.89 dB better using conventional Butterworth and integrated and dump filters, respectively. SOQPSK (0.2,2.05,1.8,0.2) requires more bandwidth than the others, but only requires 9.88 dB Eb/No to achieve a BEP of  $10^{-5}$ .

NOTES	DETECTOR TYPE Eb/No (dB) required for BEP = 10 <sup>-5</sup>				Band-width 99.99% with NLA (Bit Rates)	SOQPSK Parameters			
	Optimized Linear Filter	Viterbi	Butter -worth	Int & Dump		ρ	B	T <sub>1</sub>	T <sub>2</sub>
SOQPSK-B	10.24	9.89	10.54	11.01	1.3620	0.5	1.45	2.8	1.2
SOQPSK-A	11.05	10.50	12.12	13.04	1.2523	1.0	1.35	1.4	0.6
SOQPSK (0.7,1.25,1.5,0.5)	10.92	10.24	11.45	12.15	1.2523	0.7	1.25	1.5	0.5
SOQPSK-C (0.2,2.05,1.8,0.2)	9.88	9.63	10.08	10.46	1.5370	0.2	2.05	1.8	0.2

Table 2. Summary of SOQPSK performance

For comparison purposes, Table 3 lists the performance of some other telemetry modulation types. The best overall detection performance is achieved with IRIG PCM/FM using a multi-symbol detector. However, it requires nearly twice the bandwidth of the more spectrally efficiency SOQPSK variants. The Tier II Multi-h CPM waveform is by far the most spectrally-efficient with relatively good detection efficiency. However, since a Viterbi demodulator is required to recover the data, the demodulator complexity is much higher than for linear demodulation schemes. The SOQPSK variants offer a balance of good spectral and detection efficiency with more modest demodulator complexity. Note that if differential encoding is required to resolve the QPSK phase ambiguity, the detection performance will be degraded by approximately 0.3 to 0.5 dB from the values in the tables since the BEP approximately doubles at low error rates when differential encoding/decoding is enabled. Differential encoding is not required for either the PCM/FM or Multi-h CPM modulations.

Other Telemetry Modulation Types	DETECTOR TYPE Eb/No (dB) required for BEP = 10 <sup>-5</sup>			Bandwidth 99.99% with NLA (Bit Rates)
	Recommended Linear Filter	Viterbi	Multi- Symbol	
PCM/FM h=0.7,4 <sup>th</sup> order Bessel	11.9	-	9.35	2.4
ARTM TIER I Feher-Patented QPSK FQPSK-B	11.6 [5]	10.4 [5]	-	1.26 [6]
ARTM TIER II Multi-h CPM (M=4,L=3RC,h <sub>i</sub> =4,5/16)	-	11.17	-	0.913

Table 3. Performance of several other Telemetry Modulations

Figures 6 and 7 show the BEP curves for SOQPSK-A, -B, while Figures 8 and 9 show the performance of SOQPSK (0.7,1.25,1.5,0.5), and SOQPSK (0.2,2.05,1.8,0.2).

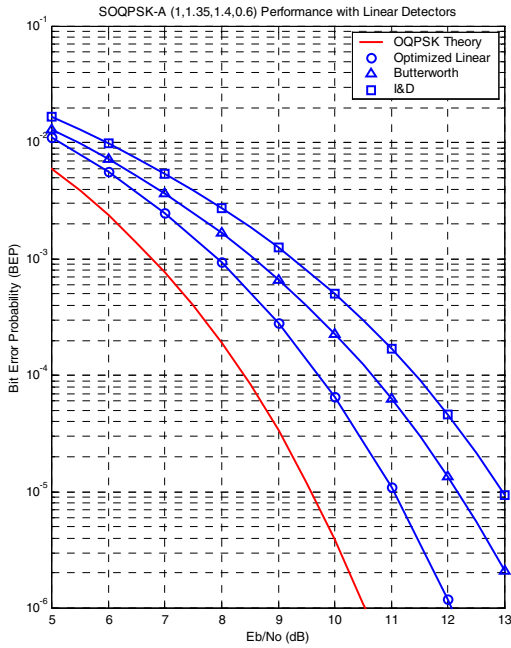


Figure 6. Linear Detection of SOQPSK-A (1,1.35,1.4,0.6) (99.99%BW=1.2523R)

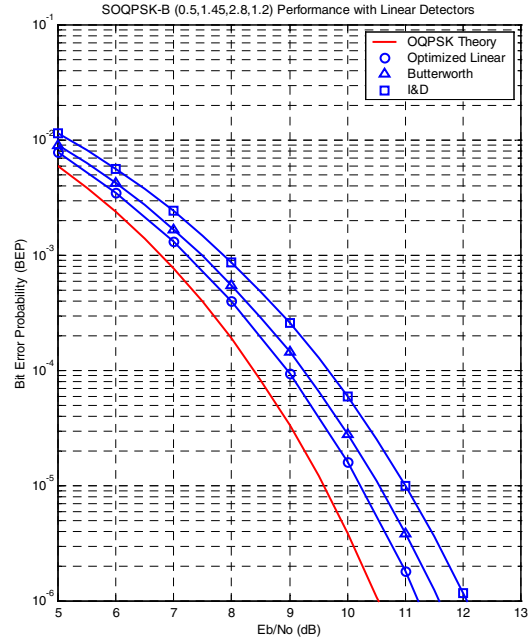


Figure 7. Linear Detection of SOQPSK-B (0.5,1.45,2.8,1.2) (99.99%BW=1.362R)

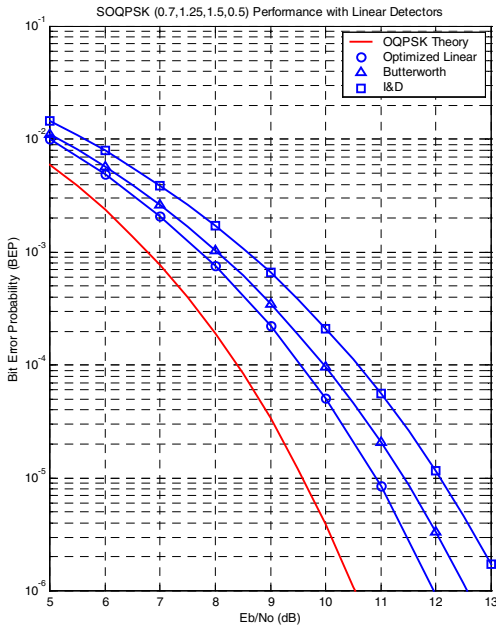


Figure 8. Linear Detection of SOQPSK (0.7,1.25,1.5,0.5) (99.99%BW=1.2523R)

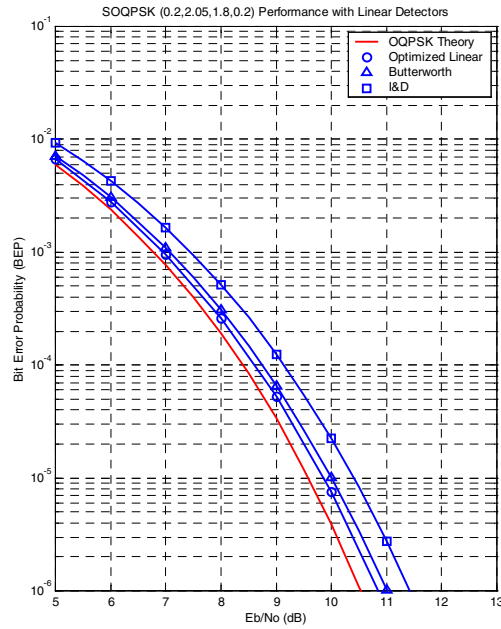


Figure 9. Linear Detection of SOQPSK (0.2,2.05,1.8,0.2) (99.99%BW=1.537R)

Figures 10 and 11 show the detection and spectral performance of selected SOQPSK variants.

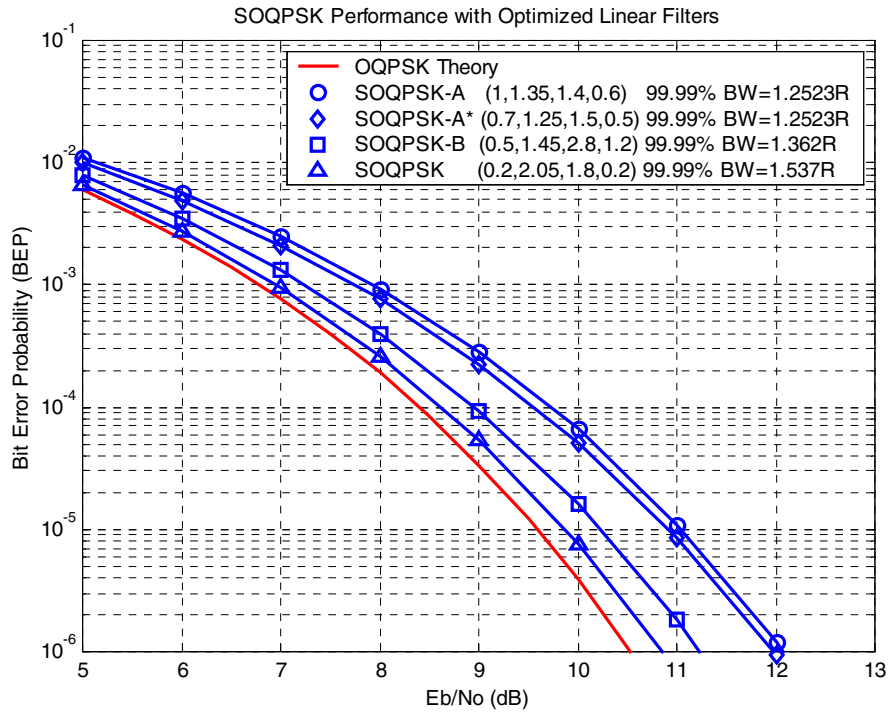


Figure 10. Performance of SOQPSK variants with Optimized Linear Filters

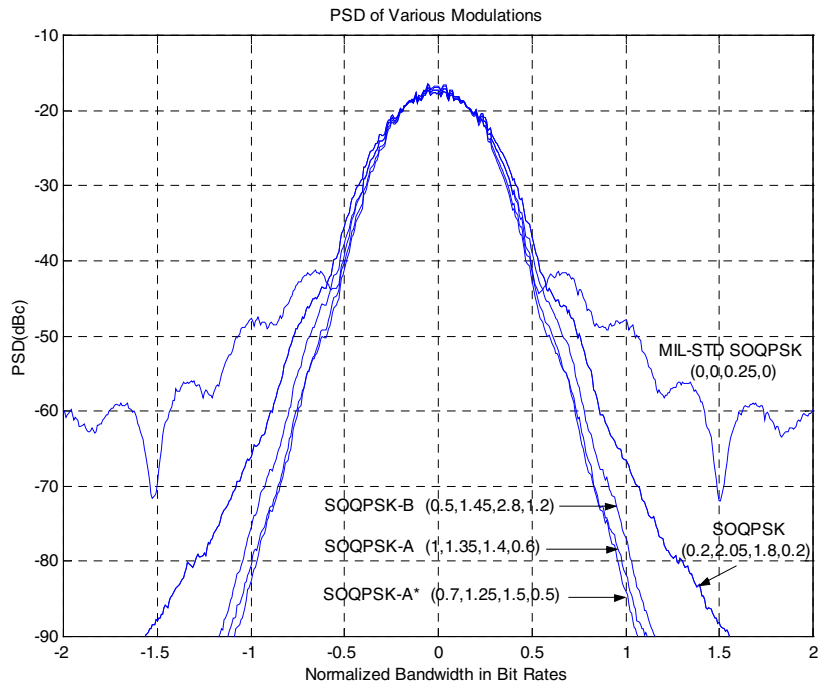


Figure 11. PSD of several SOQPSK variants

Figure 12 shows the out-of-band power and Figure 13 shows the bandwidth-power efficiency plane for several variants of SOQPSK as well as other popular modulations.

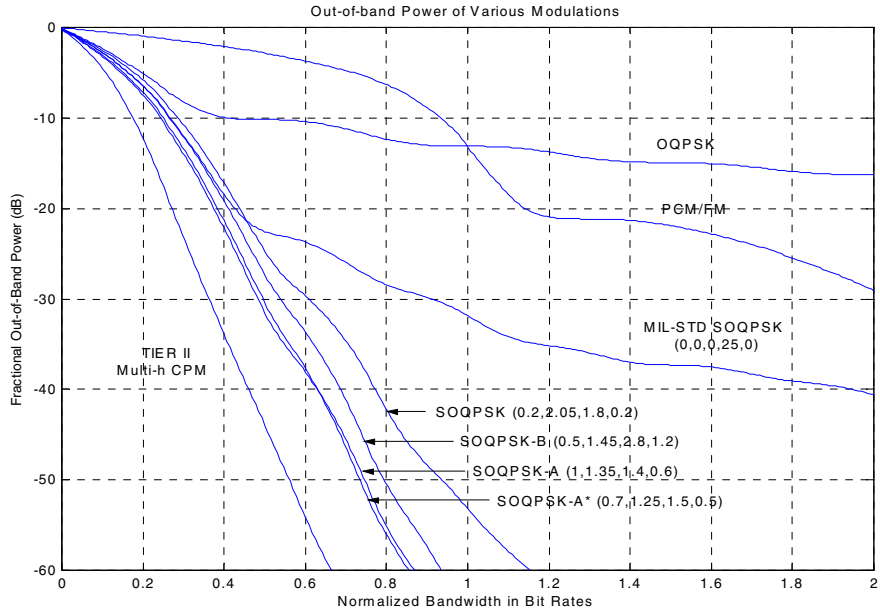


Figure 11. Out-of-Band Power of several SOQPSK variants

Bandwidth and Power Efficiency of Various Modulations (99.99% BW)

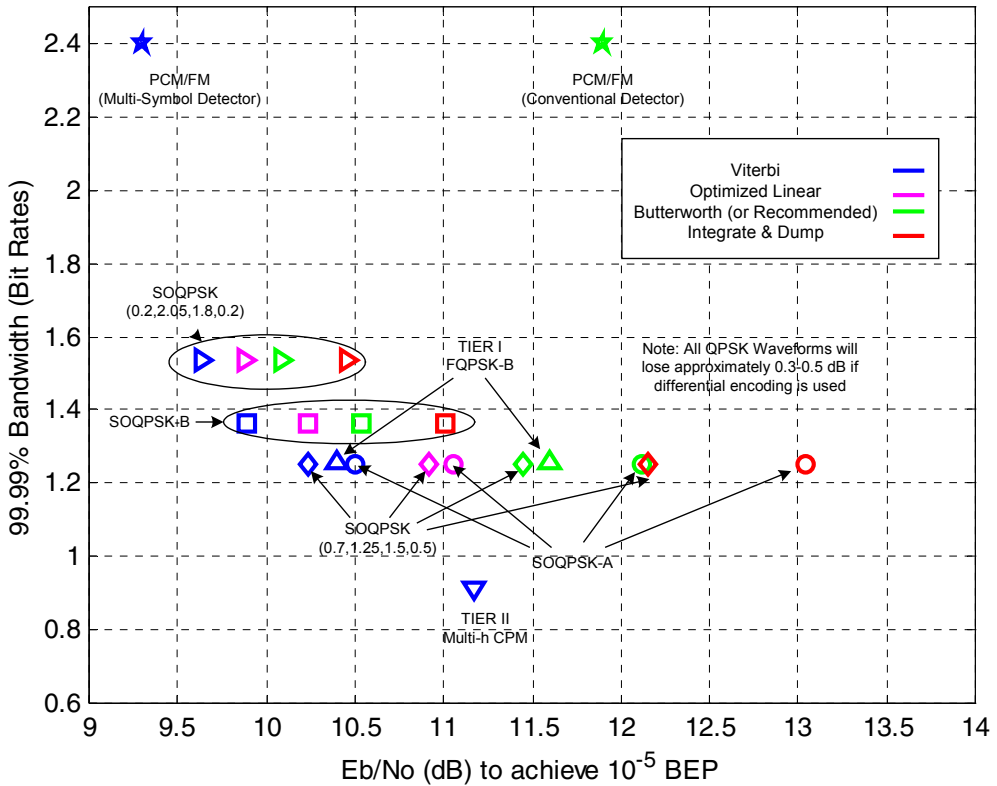


Figure 12. Bandwidth/Power Efficiency Plane with Various Modulations with NLA

## CONCLUSIONS

A linear receiver architecture for demodulating SOQPSK was presented that used an iterative technique to determine the optimal detection filter tap weights. Improvements in detection efficiency ranged from 0.2 to 2 dB as compared to the Butterworth and integrate and dump filtering typically found in conventional OQPSK equipment. In addition to SOQPSK-A and -B, results for two other members of the SOQPSK family, namely (0.7,1.25,1.5,0.5) and (0.2,2.05,1.8,0.2), were also presented. The first variant has the same spectral performance as -A but is easier to detect. The second variant requires more bandwidth than either -A or -B, but exhibits very good detection efficiency with the filtering found in conventional OQPSK detectors. An out-of-band power and bandwidth/power efficiency plot with SOQPSK and several popular modulation types were also presented. They show that SOQPSK is an attractive choice with good performance and reasonable implementation complexity. In summary, SOQPSK is a family of non-proprietary, constant envelope waveforms that have outstanding detection efficiency and spectral containment and are ideally suited for a variety of commercial and military applications.

## REFERENCES

1. T. Hill, "An Enhanced, Constant Envelope, Interoperable Shaped Offset QPSK (SOQPSK) Waveform for Improved Spectral Efficiency", Proceedings of the International Telemetry Conference, San Diego, CA, October 2000.
2. M. Geoghegan, "Implementation and Performance Results for Trellis Detection of SOQPSK", Proceedings of the International Telemetry Conference, Las Vegas, NV, October 2001.
3. B. Younes; J. Brase; C. Patel; J. Wesdock, "An Assessment of Shaped Offset QPSK for Use in NASA Space Network and Ground Network Systems", Meetings of Consultative Committee for Space Data Systems, Toulouse, France, October 2000.
4. B. Widrow and J.M. McCool, "A comparison of adaptive algorithms based on the methods of steepest descent and random search", IEEE Transactions Antenns Propag., Vol AP-24, p.615, September 1976.
5. D.Lee, M. Simon, T.Y.Yan, "Enhanced Performance of FQPSK-B Receiver based on Trellis-Coded Viterbi Demodulation", Proceedings of the International Telemetry Conference, San Diego, CA, October 2000.
6. K. Feher, R. Jefferis, E. Law, , "Spectral Efficiency and Adjacent Channel Interference Performance Definitions and Requirements for Telemetry Applications", Proceedings of the International Telemetry Conference, Las Vegas, NV, October 1999.